Performance Analysis of Direct Detection Spectrally Sliced Receivers Using Fabry–Perot Filters

Mark S. Leeson

***Abstract*—The use of a spectrally sliced (SS) broad-band source provides a cost effective alternative to laser diode sources for wavelength-division multiplexing (WDM). In this paper the performance of direct detection p-i-n diode intensity modulated SS systems is analyzed using the saddlepoint approximation. Using this approach, based on moment generating functions, the effects of pulse distortion, intersymbol interference (ISI) and nonideal modulator extinction ratios have been included in the analysis of SS systems for the first time. The presence of ISI error floors as the product of optical bandwidth and bit time decreases is demonstrated using a model that agrees with previous work in the case of low bit rate, widely spaced channels. In addition, comparisons with recent experimental results from the literature are made with good agreement. Subsequently, the use of an integrate and dump filter where the integration time starts after the beginning of a bit is investigated and shown to produce significant enhancements to bit-error rate performance. Furthermore, it is shown that a modulator extinction ratio of 20 dB will suffice for 10^{-9} bit-error rate (BER) in most cases, with 30 dB offering a performance close to that possible with an ideal modulator. Finally, the likely system power for an SS system is presented.**

***Index Terms*—Intersymbol interference, optical communication, saddlepoint approximation, spectral slicing, wavelength-division multiplexing (WDM).**

I. Introduction

WAVELENGTH division multiplexing (WDM) offers an increasingly attractive path for upgrading the digital telecommunications access network to cope with increasing customer bandwidth requirements [1]. The economic aspects of service provision in this portion of the network are such that low cost methods of generating a range of wavelengths are necessary. One option is to use an optical filter to provide narrow slices of a broad-band noise source producing an approach commonly known as spectral or spectrum slicing (SS) [2]–[5]. This provides a cost-effective alternative to laser diode sources for WDM systems but introduces excess intensity noise due to the source incoherence. To investigate the performance of SS systems it is useful to define the parameter m, given by the produce of the optical bandwidth of the SS signal (B_0) and the bit time (T). To reduce the statistical fluctuations in signal energy m should be large, but this limits the number of available WDM channels and introduces a power penalty due to fiber dispersion. The use of low m values, however, increases the number of photons per bit needed to achieve a given error rate because of the energy fluctuations in the noise like source. Additionally, as demonstrated subsequently in this paper the effect of intersymbol interference (ISI) is greatly increased as m is reduced.

Analysis of SS systems using Gaussian noise statistics is not appropriate in the regions of practical interest, that is narrow channels and high bit rates, as recently demonstrated by Arya and Jacobs [6]. To date the theoretical framework used to predict the bit-error rate (BER) performance of SS systems has not included realistic filter or modulator characteristics. The main purpose of this paper is to analyze the sensitivity of a p-i-n diode receiver using SS signals via an improved statistical model of a broad-band source and an accurate transfer function for the filter used to slice it. Additionally, it is demonstrated that care must be exercised in the approximation of the receiver optical filter by an equivalent optical bandwidth rectangular filter on two counts. First, the approximation is increasingly inaccurate at low values of m and second the use of an orthogonal function expansion for analysis requires the calculation of the exact eigenvalues rather than an equal eigenvalue approximation. Moreover, using the saddlepoint approximation (SPA) [7] described all the necessary calculations may be carried out relatively quickly using a PC. Further to this, the methods used are shown to correlate well with experimental results from the literature and to allow incorporation of nonideal extinction ratios. Also, it is demonstrated that the use of receiver integration times starting after the beginning of a bit period offers significant benefits in terms of reduced ISI. This enables the error floors due to ISI to be dramatically reduced and operation at low m values to be possible in exchange for a small power penalty at high m values.

Section II provides an outline of the receiver structure used for the analysis and presents the mathematical framework for the problem. Section III presents the SPA for the SS system assuming a rectangular receiver filter without intersymbol interference (ISI). Results are first obtained using an orthogonal expansion for the noise in which the eigenvalues are assumed to be m in number and all of equal value. It is demonstrated that this assumption is likely to be inaccurate at low m values and results obtained using the correct eigenvalues for the rectangular filter. Section IV describes the modification of the model to include Fabry–Perot (FP) filters comprising two main elements. First, the photocurrent resulting from a received pulse is reduced because of the impulse response of the FP filter. Second, ISI is present since the FP produces an exponential pulse tail, which also leads to a crossproduct (beat term) when two one pulses follow each other. The modifications to the simplified model of Section III are quite considerable, requiring nonstationary statistics to be incorporated in a manner described in the Appendix. Section V presents the results obtained using the

Manuscript received July 30, 1999.

The author is with the Department of Electronic and Computer Engineering, Brunel University, Uxbridge, Middlesex UB8 3PH, U.K.

Publisher Item Identifier S 0733-8724(00)00395-9.

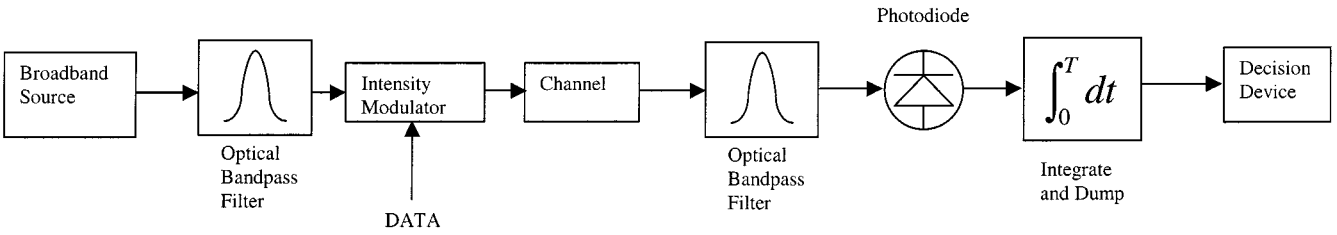

Fig. 1. The model of the spectrally sliced system considered.

improved model and also a comparison with experimental results from the literature. In Section VI the benefits of starting the receiver integration period after the beginning of a bit are investigated. This method, although studied for optically preamplified systems, has not before been examined in the context of SS systems. Section VII presents the impact of nonideal extinction ratios on the SS system to simulate the effect of practical modulators. The system implications of the performance of SS transmission are addressed in Section VIII by determination of the available power budget. The outcomes of the study are discussed in Section IX and conclusions drawn in Section X.

II. Model of the Receiver Structure

The receiver structure assumed in this analysis is shown in Fig. 1, where the incoming signal has been produced by taking a narrow slice of a noise like source. It arrives at an optical bandpass filter nominally identical to that used to produce the transmitted spectrum. The filter is followed by an ideal square law detector and an integrate and dump filter. For the case of on–off keying, considered here, the integrated pulse energy is compared with a decision threshold. In the formalism of [6], the current signal at the input to the decision circuit may be expressed as

$$I = \frac{1}{2T}\int_0^T \left[x^2(t) + y^2(t) + \tilde{x}^2(t) + \tilde{y}^2(t)\right]\, dt + I_n \quad (1)$$

where $x^2(t)$, $y^2(t)$, $\tilde{x}^2(t)$ and $\tilde{y}^2(t)$ are independently identically distributed baseband Gaussian processes with optical bandwidth $B_o/2$ and variance σ^2. This latter quantity is equal to the photocurrent contributed by each of the two orthogonal polarizations. The term I_n represents the thermal noise current induced in the electrical part of the receiver, which is much greater than shot noise (taken as negligible) for a p-i-n diode. A receiver filter is always necessary for a spectrally sliced system for wavelength-division demultiplexing (WDM) so the noise like signals, x, y, $\tilde{x}$, and $\tilde{y}$, are thus doubly filtered Gaussian processes and must be analyzed accordingly. The squaring of these processes by the photodiode renders them non-Gaussian since it is a nonlinear operation. Despite this it is still worth considering a Gaussian approximation since it leads to an analytically straightforward method. The recent results in [6] have shown, however, that such an approximation is only justified when the slicing filter bandwidth is a large multiple of the bit rate. In other cases the Gaussian approximation is far too conservative and leads also to error floors that are not present in practice. The sections below present the analysis and results of the decision problem at the detector approached using non-Gaussian statistics in the SPA. They include favorable comparisons with both the results in [6] and experimental results in addition to a proposal to improve the performance of SS systems using integrate and dump filters.

III. Saddlepoint Approximation for a Rectangular Filter

A. Equal Eigenvalues

The saddlepoint approximation (SPA) uses moment generating functions (MGF's) to produce estimates that bit errors occur. The probability that the noise alone exceeds a threshold α, denoted by $q_+(\alpha)$, is given (for a continuous distribution) by

$$q_+(\alpha) \approx \frac{\exp\left[\psi_0(s_0)\right]}{\sqrt{2\pi\psi_0''(s_0)}} \quad (2)$$

where $\psi_0(s)$ is related to the noise MGF by

$$\psi_0(s) = \ln\left[M(s)\right] - s\alpha - \ln|s|. \quad (3)$$

The parameter s_0 is the positive root of the equation

$$\psi_0'(s) = 0 \quad (4)$$

and the primes indicate differentiation with respect to s.

When a "0" arrives only the receiver thermal noise current is present, which is Gaussian and white with zero mean. Thus the appropriate function is

$$\psi_0(s) = \frac{s^2\sigma_g^2}{2} - s\alpha - \ln|s| \quad (5)$$

for a noise current power of σ_g^2 and decision threshold α.

The case of a "1" arriving adds the filtered noise-like signal with a modified chi-squared distribution [8]. The mean signal photocurrent, σ^2, is given by

$$\sigma^2 = \overline{Np}\,\eta q R_b \quad (6)$$

where

η	photodiode quantum efficiency;
q	electronic charge;
$\overline{N_p}$	mean number of photons per bit;
R_b	bit rate.

Filtered noise-like signals, such as those produced during spectral slicing, are well described by a Karhunen–Loeve expansion [9] using the eigenfunctions, $\phi_i(t)$, and eigenvalues γ_i obtained from the equation

$$\gamma\phi(t) = \int_0^T R(t-u)\phi(u)\, du \quad (7)$$

where

T bit time;

$R(\tau)$ autocorrelation function of the noise-like signal.

The parameter $m = B_oT$ is used to characterize the performance of the system. Assuming that all the eigenvalues needed for the KL expansion are the same and equal to σ^2/m yields a moment generating function (MGF) of

$$\Psi(s) = \frac{1}{\left(1 - \frac{s\sigma^2}{m}\right)^{2m}} \tag{8}$$

and hence (5) becomes, for a one received

$$\psi_1(s) = \frac{s^2\sigma_g^2}{2} - 2m \ln\left[1 - \frac{s\sigma^2}{m}\right] - s\alpha - \ln|s|. \tag{9}$$

The appropriate probability in this case is

$$q_-(\alpha) \approx \frac{\exp[\psi_1(s_1)]}{\sqrt{2\pi\psi_1''(s_1)}} \tag{10}$$

where s_1 is in this case the positive root of $\psi_1'(s) = 0$.

For equally likely ones and zeros the overall BER is found from

$$\text{BER} = \tfrac{1}{2}\left[q_+(\alpha) + q_-(\alpha)\right]. \tag{11}$$

In [6] a threshold of $6\sigma_g$ is suggested based on the integral of the thermal noise alone with no pulse. Initially this assumption was adopted leading to a simple quadratic equation from $\psi_0'(s) = 0$ for s_0. To find a value for s_1 was only marginally more difficult requiring numerical solution of $\psi'_1(s) = 0$ from (9).

For the purposes of comparison the same values of σ_g (255 nA), η (0.7), and R_b (5 Gb/s) as [6] were used, giving the results shown by the dash-dot line in Fig. 2, where the mean number of photons required for a 10^{-9} BER is shown. The results obtained are very similar those shown in [6, Fig. 2] but the method employed here is extremely fast producing each of the results plotted in a less than a minute on a 350-MHz Pentium PC for any value of m.

B. A More Accurate Calculation

The approximation of the eigenvalues by m equal values is likely to be inaccurate for low values of m. It relies on a signal passing undistorted through a receiver filter [10] and this assumption will break down as the filter bandwidth narrows. To obtain more accurate results it is necessary to use a KL expansion with the eigenvalues taking on appropriate values for the particular filter transfer function. The function $\psi_0(s)$ remains the same but $\psi_1(s)$ becomes

$$\psi_1(s) = \frac{s^2\sigma_g^2}{2} - 2\sum_{i=1}^{\infty} \ln[1 - s\gamma_i] - s\alpha - \ln|s| \tag{12}$$

where γ_i are the eigenvalues of the bandpass filter. This is the expression recently given by Monroy and Einarsson [11] with

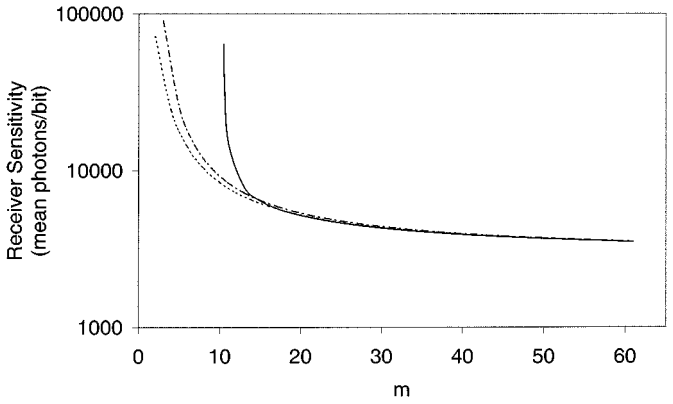

Fig. 2. Receiver sensitivity at $P_e = 10^{-9}$ using the parameters of [6] calculated by the equal eigenvalue approximation (chain line), via the exact eigenvalues for a rectangular filter (dotted line) and for the FP filter (solid line).

no signal present in an optically preamplified direct detection receiver.

The eigenvalues for the bandlimited spectrum are the radial prolate spheroidal functions [9] and may easily be found by numerical solution of (7) using the kernel $\sin(\pi B_0\tau)/\pi B_0\tau$. The number of dominant eigenvalues is known to be $m+1$ [9] and this is demonstrated by two different values of m shown in Fig. 3(a) and (b). The former illustrates a case of large m, namely 40, and the error introduced by neglecting the 41st and subsequent eigenvalues will be small. In contrast the latter illustrates the inaccuracy introduced by the equal eigenvalue assumption for $m = 2$. Here the contribution of the third eigenvalue is not negligible and the second one is significantly smaller than the first, so the use of equal eigenvalues is very inaccurate.

A direct numerical solution of $\psi'_1(s) = 0$, with $\psi_1(s)$ from (12) and a threshold of $6\sigma_g$, gave the results plotted using the dotted line in Fig. 2. To enable solution of (12), and subsequent similar expressions, truncation of the infinite sum was used with 250 eigenvalues being calculated. Although this may appear rather large, Lawetz and Cartledge [12] have demonstrated that a large number of eigenvalues are necessary for the FP case and the computational burden in the SPA was not excessive.

The graph clearly demonstrates the impact of the equal eigenvalues approximation on the number of photons required to achieve a 10^{-9} BER. At high values of m the results are very close but for low m the mean number of photons required is considerably overestimated. Given that low m represents closely spaced channels at high bit rates, the use of the equal eigenvalue approximation is insufficiently accurate for the determination of system performance limits.

The use of the threshold $6\sigma_g$ was found to be reasonable by comparison with a solution for s_0, s_1, and α by Newton's method in the manner suggested in [7]. Using the optimum threshold made only a small impact on the number of photons required to achieve 10^{-9} BER ($\overline{N}_p$ reduced by 2%–5%). The actual thresholds obtained were within a few percent of $6\sigma_g$ over the range m considered. In the calculations of Sections IV–VII below, however, the optimum threshold was determined because the ISI dominated, low m, cases required thresholds much greater than $6\sigma_g$ to optimize BER performance.

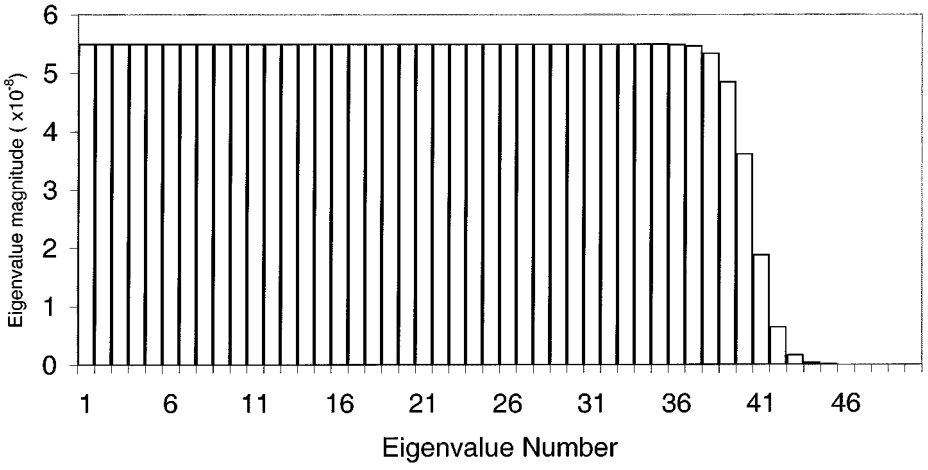

(a)

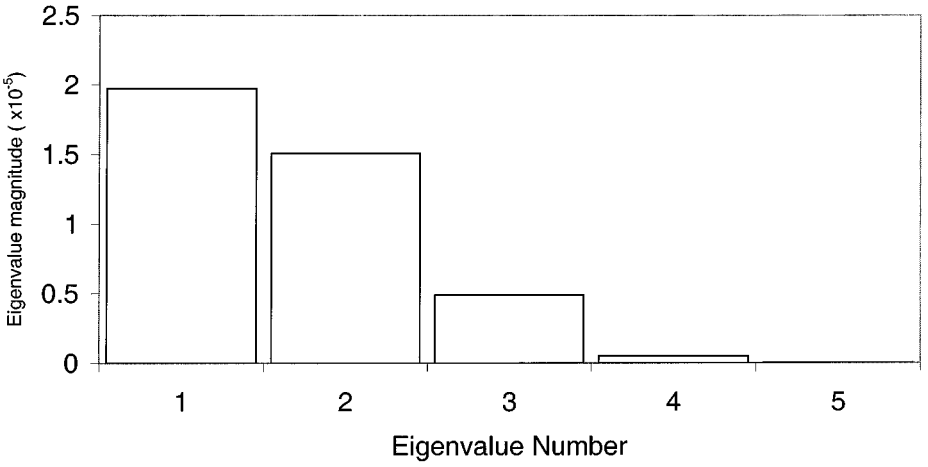

(b)

Fig. 3. The eigenvalues for rectangular filters: (a) at $m = 40$ and (b) at $m = 2$.

IV. Saddlepoint Approximation for a Fabry–Perot Filter

A. Autocorrelation Function and Signal Shape

At this stage the unrealistic assumption of a rectangular filter transfer function was laid aside in favor of the FP filter. This is a common choice for optical filtering (either in fiber or bulk form) and the receiver and transmitter were assumed to use filters with identical characteristics. Spectral slicing takes the output of a broad-band optical source [modeled by white Gaussian noise of two-sided power spectral density (PSD) $N_0/2$] and filters this to produce a narrow slice. The noise remains Gaussian but is no longer white since the PSD is modified by filtering. For high mirror reflectivities FP filters may be modeled by a Lorentzian characteristic and the equivalent baseband form of a low pass filter characteristic used with the single-sided PSD [12], [13]. The low-pass filter has transfer function

$$H(f) = \frac{1}{1 + j\left(\dfrac{f}{f_0}\right)} \tag{13}$$

where f_0 is the 3 dB bandwidth of the filter (the full-width at half-maximum (FWHM), $B_{\rm FP}$, is then $2f_0$). The received excess noise component of the spectrally sliced signal, $n(t)$, will have been filtered at both the transmitter and the receiver and thus has a PSD of

$$S_n(f) = |H(f)|^4 N_0 \tag{14}$$

hence an autocorrelation function

$$R(\tau) = \frac{\pi N_0 B_{\rm FP}}{4}\left[1 + \pi|\tau| B_{\rm FP}\right] e^{-\pi|\tau| B_{\rm FP}}. \tag{15}$$

To enable meaningful comparison of the performance of two FP filters with the idealized situation use must be made of the equivalent bandwidth [14], which is given by

$$B_o = \frac{\left[\displaystyle\int_{-\infty}^{\infty} S_n(f)\, df\right]^2}{\displaystyle\int_{-\infty}^{\infty} S_n^2(f)\, df} = \frac{2\pi B_{\rm FP}}{5}. \tag{16}$$

Additionally the pulse shape, assumed rectangular when it reaches the receiver, is distorted by the FP filter producing nonstationary signal statistics. To develop the KL expansion, a kernel must be found for the eigenvalue equation. The received pulse has a shape that will be the result of filtering by one FP because it arises from on–off keying (OOK) after the slice is

obtained. The received "1" pulse, $s(t)$, is thus, for an ideal extinction ratio

$$s(t) = \begin{cases} \left(1 - e^{-\pi B_{\rm FP} t}\right) & 0 \le t \le T \\ \left(1 - e^{-\pi B_{\rm FP} T}\right) & t > T \end{cases} \tag{17}$$

and the statistics in question are given by $n_1(t) = s(t)n(t)$. The KL expansion does not rely on the stationarity of $n_1(t)$ and, as shown in the Appendix, the relevant kernel is

$$K_{n_1}(t, u) = \sigma^2 \left(1 - e^{-\pi B_{\rm FP} t}\right) \left(1 - e^{-\pi B_{\rm FP} u}\right) \times [1 + \pi |t - u| B_{\rm FP}]\, e^{-\pi |t-u| B_{\rm FP}}. \tag{18}$$

B. The Photodiode Output

The intersymbol interference (ISI) resulting from the exponential decay in (17) above has been the subject of study of this author and others [15]–[18] but not in the context considered here. The only previous consideration of the performance of SS systems with nonrectangular filters by, Arya [19], does not include ISI and will thus be optimistic

$$I = \begin{cases} \dfrac{1}{2T} \displaystyle\int_0^T [s(t)n(t) + \mathrm{ISI}(t)]^2 \, dt + I_n & \text{"1" received} \\ \dfrac{1}{2T} \displaystyle\int_0^T [\mathrm{ISI}(t)]^2 \, dt + I_n & \text{"0" received.} \end{cases} \tag{19}$$

By using the variable $n_1(t)$ it is possible to produce a KL expansion for the noise like signal to play the role of the second term in (12). In the Appendix it is shown that the ISI may be included to a good approximation by consideration of only 1 previous pulse and that the crossproduct between $n_1(t)$ and $\mathrm{ISI}(t)$ has an approximate MGF

$$F_X(s) \approx 1 + (\sigma_1 \sigma_2)^2 \frac{s^2}{2} \tag{20}$$

where σ_1 and σ_2 are related to σ in the manner demonstrated in Section C of the Appendix. Given these approximations the ISI appears only when the previous pulse is a "1" and the crossproduct only when the current and previous pulses are both "1." Thus the SPA uses the condition (11) plus the four equations

$$\psi_{00}(s) = \frac{s\sigma_g^2}{2} - \alpha s - \ln|s| \tag{21a}$$

$$\psi_{01}(s) = \frac{s\sigma_g^2}{2} - 2\ln(1 - 2k_{\rm ISI}\sigma^2 s) - \alpha s - \ln|s| \tag{21b}$$

$$\psi_{10}(s) = \frac{s\sigma_g^2}{2} - 2\sum_{i=1}^{\infty} \ln(1 - s\gamma_i) - \alpha s - \ln|s| \tag{21c}$$

$$\psi_{11}(s) = \frac{s\sigma_g^2}{2} - 2\sum_{i=1}^{\infty} \ln(1 - s\gamma_i) + 4\ln\left(1 + (\sigma_1\sigma_2)^2 \frac{s^2}{2}\right) - 2\ln(1 - 2k_{\rm ISI}\sigma^2 s) - \alpha s - \ln|s| \tag{21d}$$

where

$\psi_{\alpha\beta}(s)$	SPA phase function for symbol α preceded by symbol β;
γ_i	eigenvalues obtained using the kernel (18);
$k_{\rm ISI}$	$(1/10m)(1 - e^{-2.5m})^2(1 - e^{-5m})$.

The form of the SPA expressions means that, in contrast to Section III, the equations are not stable for a solution using the matrix form of Newton's method. Hence the equations in (21) were solved simultaneously and standard numerical techniques[1] used to find the value of α that gave the minimum BER. Although this increased the amount of computation required, solution was still easily obtainable in a few minutes using a 350-MHz Pentium PC.

V. Results for FP Filter Spectrally Sliced System

A. Bit-Error Rate

The presence of ISI introduces floors in the achievable minimum BER for a given m. Hence, in this section the first results from the calculations above, shown in Fig. 4, are BER against mean photons per bit with m as a parameter to indicate this behavior. Note that in this section m remains the product of the bit time and the bandwidth of the ideal filter. This need not be an integer since the probability density function (pdf) for the noise like source [4] contains a gamma function in general which is replaced by a factorial when integer m values are used *for mathematical convenience*. From the figure it may easily be seen that the error floors are extremely severe for low values of m. Indeed it is not possible to achieve a BER below 10^{-9} when m is 10 or less. This is illustrated by the solid line on Fig. 2, which shows error floor behavior with the number of photons required to achieve 10^{-9} BER rising steeply to infinity as m approaches ten. This is a highly significant result, indicating that there is an absolute limit on a simple spectrally sliced system in terms of channel spacing and bit rate to achieve a given BER.

B. Comparison with Published Results

As indicated by Arya and Jacobs [6] there is a lack of experimental data for spectrally sliced systems at low m values. One of the most useful recent practical contributions has been made by Keating and Sampson [4] and here comparison is made with their results for the standard SS system. To undertake the comparison an avalanche photodiode (APD) was incorporated into the model using the approach of [7]. In essence the MGF is modified to take account of the shot noise within the APD and its gain (M) to become, for each orthogonal component

$$\Psi_{\rm APD}(s) = \prod_{i=1}^{\infty} \frac{1}{\sqrt{1 - \gamma_i \left(\Psi_a(s) - 1\right)}} \tag{22}$$

where $\Psi_a(s)$ is the MGF of the avalanche gain, given by Personick's relationship [20]. The use of $(\Psi_a(s) - 1)$ in the MGF corresponds to the customary Poisson transform [7] to account for the doubly stochastic Poisson statistics within the APD. Modeling carried out in [4] used the Gamma distribution

[1]All the calculations in this paper were performed using MATLAB®.

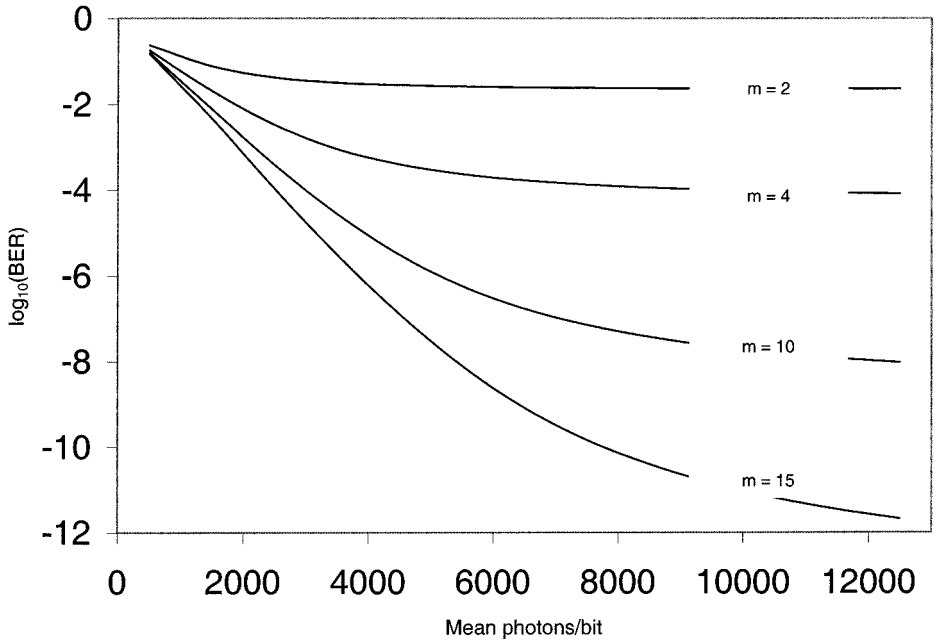

Fig. 4. The logarithm of the BER as a function of the received photons per bit for m values between 2 and 15.

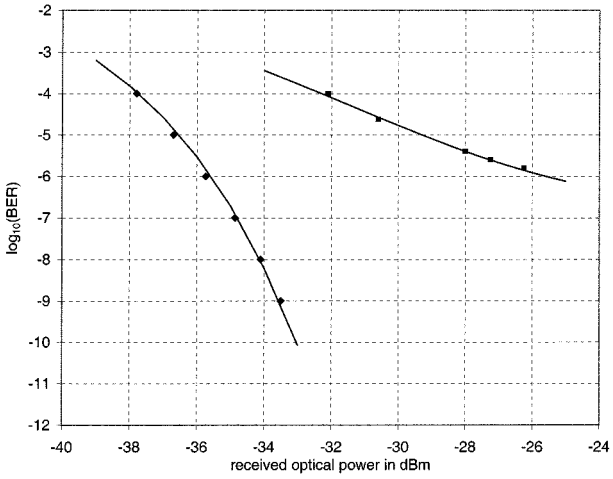

Fig. 5. Comparison of calculated results (solid lines) with the experiment of Keating and Sampson [4] (diamonds) for: (a) a laser diode and (b) an SS source.

for in which the statistics of x, the optical power received, are given by

$$p_x(x) = \left(\frac{\mathrm{SNR}_x}{\mu_x}\right) x^{\mathrm{SNR}_x - 1} \frac{\exp\left(-x\dfrac{\mathrm{SNR}_x}{\mu_x}\right)}{\Gamma(\mathrm{SNR}_x)}, \quad (\mathrm{SNR}) \tag{23}$$

where μ_x is the mean value of x and

$$\mathrm{SNR}_x = \frac{pB_0}{2B_e} \tag{24}$$

with

B_0 equivalent bandwidth of (16) above;
B_e electrical noise equivalent bandwidth;
$p = 1(2)$ polarized (unpolarized) light.

Equation (23) represents the pdf corresponding to the MGF in (8) when an unpolarized source and an integrate and dump filter are used. This may be seen by substituting $B_e = 1/2T$ into (24) for the integrate and dump filter to give $\mathrm{SNR}_x = 2m$, $\mu_x = 2\sigma^2$ and recognizing that $\Gamma(2m) = (2m-1)!$ for integer m. Keating and Sampson's experiment used a polarizer so $\mathrm{SNR}_x = m$ and $\mu_x = \sigma^2$, leading to an MGF equivalent to the rectangular filter approximation, namely

$$\Psi(s) = \frac{1}{\left(1 - (\Psi_a(s) - 1)\,\dfrac{\sigma^2}{\mathrm{SNR}_x}\right)^{\mathrm{SNR}_x}} \tag{25}$$

including the APD. For further validation and comparison, the standard case of a laser source was incorporated the framework by removing the excess noise MGF. One further refinement was required in that a nonideal extinction ratio had to be incorporated to account for the characteristic of the Mach–Zehnder modulator used in [4]. The result of this was that there was no longer a state where zero photons arrive and both SPA functions contained functions of the form (22) with different eigenvalues for "0" and "1." For extinction ratio ε, N_1 photons were assumed to arrive during a "1" pulse and $N_0 = N_1/\varepsilon$ photons in a "0," resulting in a mean number $N_1(1+\varepsilon^{-1})/2$ of photons per bit. The necessary parameters for the APD were assigned typical values for an InGaAs device [21], a center wavelength of 1534 nm was used for the FP and the laser was assigned a realistic wavelength of 1560 nm. The best fit was obtained by allowing the APD quantum efficiency and gain to be slightly different for the laser and the SS. This is likely for different wavelengths and also it is possible that the APD and modulator exhibited some nonlinearity. Fig. 5 shows a comparison of the calculated $\log_{10}$(BER) as a function of received power, using the parameters shown in Table I, for the SS and laser compared with points taken from [16]. The agreement is very good, given that all diode parameters had to be estimated, with the extinction ratio and SNR used being only 1.5 and 1 dB away, respectively, from those quoted for the experiment.

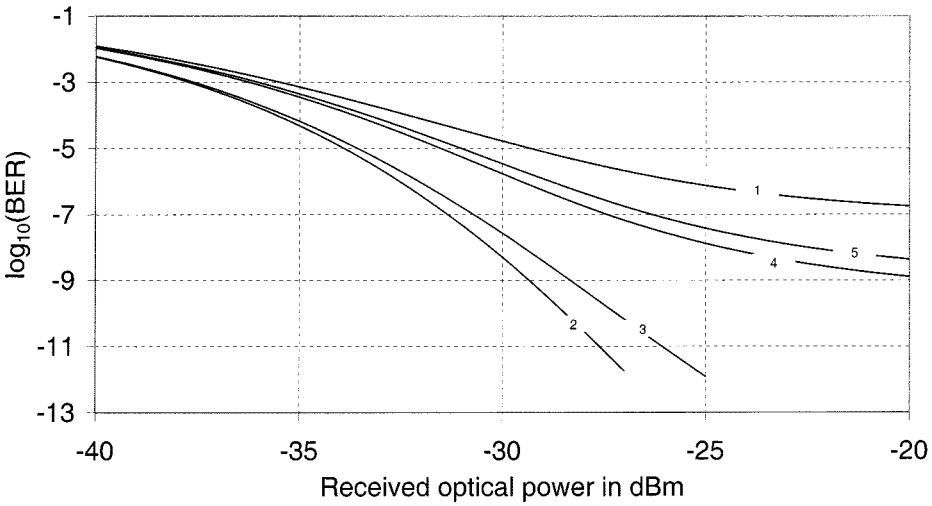

Fig. 6. Extensions to the calculations of Fig. 5. 1—calculated results for the experiment of [4]; 2—integrate and dump with SNR$_x$= 37; 3—(25) with SNR$_x$= 37; 4—integrate and dump with SNR$_x$= 14; and 5—2 FP system with $m \approx 15$.

TABLE I
PARAMETERS USED IN COMPARISON OF CALCULATED RESULTS WITH THE EXPERIMENT OF KEATING AND SAMPSON [4]

Parameter	Value for Laser	Value for SS	Units
APD ionisation coefficient ratio, k	0.65	0.65	-
APD gain M_{APD}	34	39	-
Dark Current	5	5	nA
Quantum Efficiency	0.72	0.69	-
Wavelength	1560	1534	nm
Thermal Noise Current	250	250	nA
Extinction Ratio	13	13	dB
SNR_x	-	11.5	dB
Bit Rate	2.5	2.5	Gbps

To quantify the benefit of an integrate and dump filter the MGF in (25) was replaced with one including the eigenvalues for the FP filter, namely

$$\Psi(s) = \prod_{i=1}^{\infty} \frac{1}{(1-(\Psi_a(s)-1)\gamma_i)}. \tag{26}$$

The value of m for a straight substitution in the experiment of [16] was 37, since the nominal experimental $B_{\rm FP}$ was 0.23 nm at 1534 nm. Such a high value of m produced dramatic changes in BER, as may be seen from curve 2 on Fig. 6. Comparison with the fit to the experimental SS results, reproduced as curve 1, shows several dB's improvement for all BER's and removal of the error floor. Such a comparison is not the most useful one because increasing m, which is effectively SNR$_x$, is bound to give much improved performance. This is demonstrated by curve 3 which shows the result of a calculation based on (25) but using SNR$_x$ $= 37$. Again, vastly improved performance is demonstrated but the integrate and dump offers an advantage of a few dB's. A better approach is thus to view the use of the integrate and dump filter as a way of either increasing the available bit rate per channel or permitting closer channel spacing by virtue of smaller FP bandwidths being possible. To demonstrate this curve 4 shows the BER of an integrate and dump based system with SNR$_x$= 11.5 dB $(m = 14)$ to match the experimental fit. A considerable improvement in performance is shown with the error floor reduced by two orders of magnitude.

Note that the experimental arrangement fed the output of the modulator straight to the APD, there was no receiver filter and no ISI. This system would not be satisfactory for WDM so once good agreement with the measured results had been obtained the analysis was extended to examine the likely performance of such a system for WDM. The eigenvalues from the kernel (18) were used in (26) and ISI included (the crossproduct was neglected as it is negligible for the m values relevant in this section). The double FP combination resulted in $m \approx 15$ and a BER performance shown by curve 5, which is only slightly degraded in comparison with curve 4. This is a promising result since it represents the arrangement that would be needed for an operational WDM system.

VI. REDUCED INTEGRATION TIME

Two particularly promising proposals have been considered to date to improve the performance of SS transmission systems, namely, optical preamplification [6] and feedforward noise reduction [16]. Here a simpler option is considered, requiring no additional optical components. The integration time $(T_{\rm int})$ is adjusted so that it starts from some time, T_s, greater than zero. This will considerably ameliorate the effects of the ISI while not significantly reducing the integrated output until T_s becomes a large fraction of T.

The benefit likely to be obtainable by using a reduced integration time was investigated in several ways. Initially the likely starting point for integration was examined by calculating the growth of the power received in the bit and the ISI, normalized to their respective maximum values. The former was found by using the kernel (18), calculating the eigenvalues resulting from changing the limits of integration from $[0, T]$ to $[T_s, T]$ and then

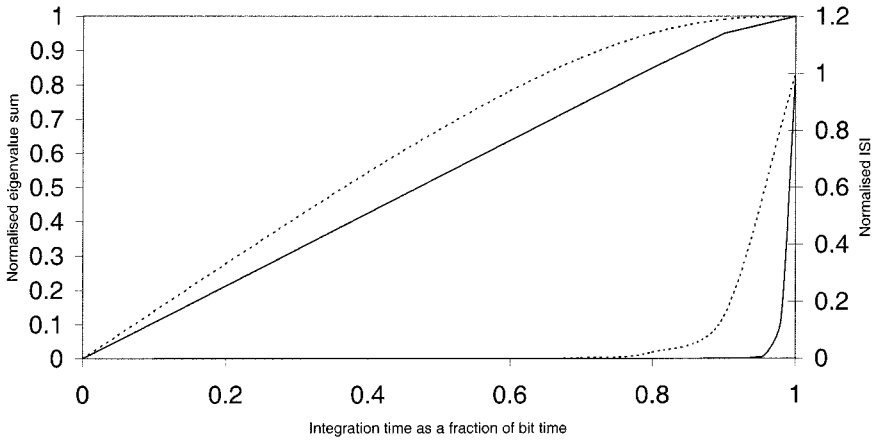

Fig. 7. Normalized eigenvalue sum (left hand scale) and normalized ISI (right hand scale) as a function of integration time for $m = 2$ (dotted line) and $m = 10$ (solid line).

taking their sum. To find the latter the multiplier $k_{\rm ISI}$ was modified to take account of the changed integration time and became

$$k_{\rm ISI} = \left(\frac{1}{[1 - T_s/T]}\right)\left(\frac{1}{10m}\right)\left(e^{-2.5m(T_s/T)} - e^{-2.5m}\right)^2 \times \left(e^{-5m(T_s/T)} - e^{-5m}\right). \quad (27)$$

Fig. 7 shows the variation of the eigenvalue sum and ISI for a low m value of 2 and for a mid range value of 10. It is apparent that the ISI is mostly confined to the first 10%–20% of the bit. Thus by reducing the integration time to 80%–90% it is possible to greatly reduce ISI while still capturing the majority of the power in a one pulse, which is at 80% or more of its maximum for such integration times.

To further quantify the effects of integration time a modified crossproduct term was included. For this the variance of the nonstationary component became

$$\sigma_1^2 \approx \frac{0.12e^{-5m(T_s/T)}}{m^2} \times \left[1 - 1.06e^{-2.5m(T_s/T)} + 0.3e^{-5m(T_s/T)}\right]\sigma^2. \quad (28)$$

The integration time was varied from 75% to 100% of the bit time for different values of m and received photons. The outcome may be summarized with reference to Fig. 8, which shows the variation in BER with $T_{\rm int}$ for the m values of five and ten at two different numbers of mean received photons per bit. There is an optimum value for the integration time to achieve the lowest BER, where the benefits of ISI amelioration are not outweighed by the loss of collected power. The optimum moves to higher percentages of the bit time as m increases since the ISI becomes less significant so the impact of collected power loss rapidly dominates. The minima are quite flat, however, suggesting that benefits are easy to obtain by control of the integration period requiring only modest precision. The impact on the performance of SS system using the reduced integration time may be demonstrated by the results shown in Fig. 9. This shows the mean number of photons per bit needed to achieve 10^{-9} BER as a function of m and using $T_{\rm int}$ as a parameter. Comparison with Fig. 2 reveals that the range of m for which the

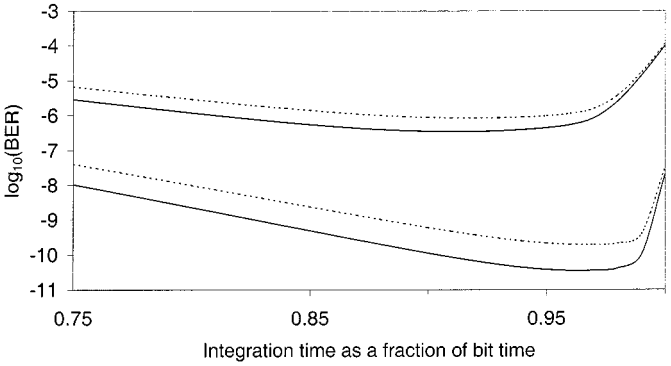

Fig. 8. Logarithm of the BER as a function of integration time for $m = 5$ (upper curves) and $m = 10$ (lower curves) at $\overline{N_p} = 9000$ (dotted lines) and $\overline{N_p} = 10\,000$ (solid lines).

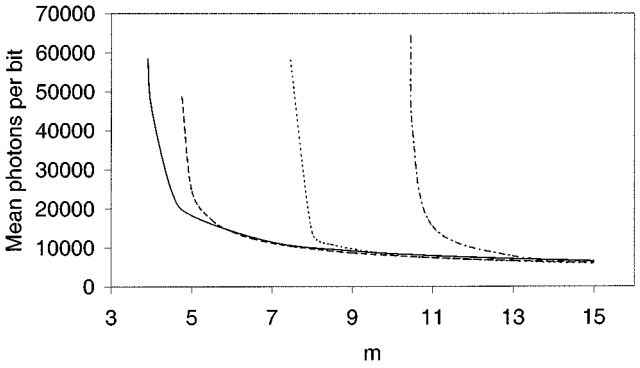

Fig. 9. Receiver sensitivity at $P_e = 10^{-9}$ using the parameters of reference [6] calculated for $T_{\rm int} = T$ (chain line); $T_{\rm int} = 0.99T$ (dotted line); $T_{\rm int} = 0.95T$ (dashed line); and $T_{\rm int} = 0.9T$ (solid line).

desired BER may be obtained is considerably extended. The reduced integration time removes the error floor but price paid for this is power penalty of up to 1 dB as m gets large.

VII. Impact of Extinction Ratio

The results in the preceding sections, apart from Section V-B, all assume an ideal extinction ratio. As shown, however, by the comparison with experimental results above this is not altogether realistic and extinction ratio will play a part in the performance achievable in SS systems. The effect of a nonideal

extinction ratio will be particularly noticeable for low values of m, where the ISI is already producing an error floor. This was investigated by calculating the BER achieved as a function of the mean number of photons received using the extinction ratio, ε, as a parameter. The SPA equations were modified using the same approach as Section V-B above and took on a form similar to (21d), since there was always a photocurrent present. The four cases arising from the use of one previous bit were incorporated by the use of the appropriate photocurrents for the signal, ISI and crossproduct.

Typical results are shown in Fig. 10 for $m = 5$ with other parameters being the same as used in Sections II–IV. The dotted lines represent the use of the whole bit for integration, for comparison with Fig. 4, while the solid lines represent $T_{\rm int} = 0.9T$. The benefit of the reduced integration time may clearly be seen as is the effect of a low extinction ratio. The results with an infinite extinction ratio are not shown on the figure because they would be indistinguishable from the 30 dB results.

In addition the problem was addressed from the angle of ascertaining the minimum extinction ratio that will permit a particular error rate to be achieved. Fig. 11 shows the necessary extinction ratios as a function of m for BER's of 10^{-9} and 10^{-6} using a 90% integration time. The figure shows illustrative results for mean numbers of photons received of 20 000 and 15 000 but the effects were similar for all signal levels. Examination of the figure shows that an extinction ratio of 20 dB or better will allow operation down to the minimum m set by the ISI.

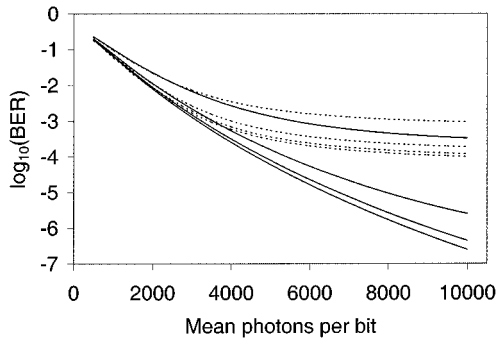

Fig. 10. The logarithm of the BER as a function of the received photons per bit for $m = 5$ with extinction ratios of 10, 15, 20, and 30 dB; solid lines $T_{\rm int} = 0.9T$ and dotted lines $T_{\rm int} = T$.

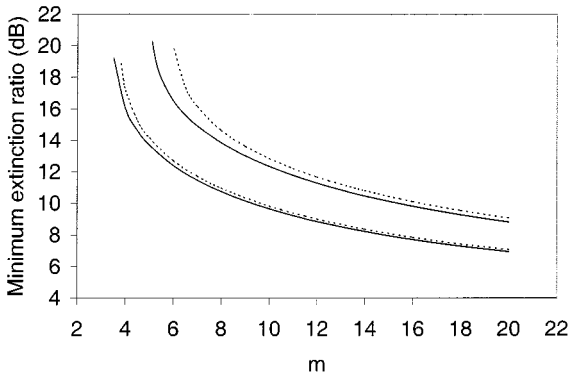

Fig. 11. The minimum extinction ratio required to achieve a BER of 10^{-9} (upper curves) and 10^{-6} (lower curves) as a function of m for $\overline{Np} = 20\,000$ photons per bit (solid line) and 15 000 photons per bit (dotted line); $T_{\rm int} = 0.9T$.

VIII. System Implications

In this section the results from the above sections are used to make an assessment of the power budget likely to be available. True determination of the system limits needs definite parameters to be meaningful since if, for example, a physical layer BER of 10^{-6} is acceptable and a power budget of 20 dB will suffice then the total capacity will be hundreds of gigabits per second. Such high figures may indeed be possible but the exploration of the full space of system possibilities is not the focus of this paper. With this caveat it is instructive to compare the available power budget as a function of the optical bandwidth per channel.

The power budget may be obtained using the ratio (expressed in dB's) of the mean number photons that would be received by a photodiode straight in front of the transmitter to the mean number actually required to achieve 10^{-9} BER. By equating the power received and the power in the slice just after the transmitter the following is obtained for the number of transmitted photons per bit, $\overline{N_{pT}}$

$$\overline{N_{pT}} = \frac{\pi B_{\rm FP} N_0}{2h\nu R_b} \tag{29}$$

where

h Planck's constant;
ν frequency of the light;
N_0 PSD of the broad-band source.

Using the PSD of Sampson and Holloway [3], namely 3.2×10^{-14} W/Hz at 1550 nm, and a per channel bit rate of 2.5 Gb/s permits immediate comparison with the p-i-n diode results

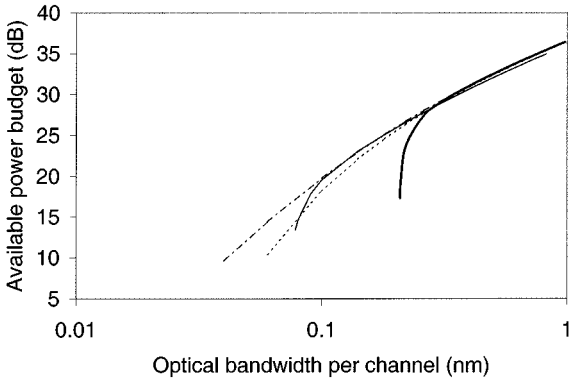

Fig. 12. Available power budget as a function of optical bandwidth per channel calculated using the method of [6] (dotted line); the eigenvalues of the rectangular filter (chain line); the eigenvalues for 2 FP filters with $T_{\rm int} = T$ (heavy solid line) and $T_{\rm int} = 0.9T$ (solid line).

of [6]. Substituting the equivalent bandwidth and inserting these values into (29) gives $\overline{N_{pT}} \approx 330\,000m$ as the maximum number of transmitted photons. Using this relationship power budgets as a function of filter bandwidth for four cases were be obtained as shown in Fig. 12, which uses a logarithmic x-axis to emphasis subsequent comments. The first case, shown in bold, is the use of two matched FP filters and $T_{\rm int} = T$; here the available power budget falls steadily from 35 dB at a filter bandwidth of 1 nm to 29 dB at 0.3 nm before a rapid

decline as the ISI limit sets in. Reduction of the integration time is the second scenario, shown as the lighter solid line; it may be seen that there is a penalty of approximately 0.5 dB at large bandwidths but the rapid decline due to ISI does not set in until 0.1 nm. The third set of results, shown as a chain line, indicates the behavior of the system predicted using the rectangular filter approximation with exact eigenvalues as in Section III-B. Finally, the equal eigenvalue approximation of [6] is shown a dotted line using the results of Section III-A. It is easy to see that these methods give the same result as the filter bandwidth increases, allowing for the small penalty incurred by the reduced integration time. This is as expected because ISI becomes a large problem only for low values of m. The main benefit of the reduced integration time is illustrated by this figure with the lower limit of operation being extended to 0.1 nm before the power budget rapidly disappears.

IX. Discussion

The use of the SPA is extremely effective in determining the BER of SS systems, for which the Gaussian approximation is overly conservative unless m is very high. At m values greater than 20 the equal eigenvalue approximation produces an error in the number of photons required for 10^{-9} BER of 0.04 dB or less (compared with the FP calculation). In contrast the Gaussian approximation produces an error of some 7.2 dB at $m = 20$, not falling below 1 dB until m is greater than 40. The ease of solution of the equations in Section III-A means that the equal eigenvalue method provides a useful BER performance estimate for $m > 20$. For m values below 20 then the accuracy of the equal eigenvalue method decreases rapidly, reaching an underestimate of 2.7 dB at $m = 11$. There seems to be, however, little benefit in using the exact eigenvalues for the rectangular filter since the region of the greatest difference in results is for low m values and the ISI error floor results presented above render the results meaningless. To obtain useful performance predictions for low m it is essential to include the effect of ISI, which eventually becomes the dominant limiting factor. This point has not emerged in previous work since it quite possible to operate with only a slicing filter in a single channel study.

For low m the neglect of the ISI and, to lesser extent, the crossproduct coupled with the leakage of power from the current bit interval, makes more detailed analysis necessary. Inclusion of both transmitter and receiver FP filters means that the noise must be treated as the output of 2 FP filters in series while the received pulse shape is the result of a single filter. The use of the equivalent optical bandwidth enables a meaningful comparison to be made between the results for 2 FP filters and for the idealized rectangular filter.

The analysis presented here is a new approach to the problem in that the KL expansion is based on a kernel appropriate to nonstationary statistics. This presents no computational problems in addition to the determination of the eigenvalues that is necessary for any analysis based on a KL expansion. The BER results obtained by the expansion tend smoothly toward those obtained from the more approximate models as m increases.

The ISI is straightforward to incorporate into the SPA since it is not necessary to carry out convolutions for additional noise and interference using an MGF based approach. The squaring operation at the photodiode means that the truncated pulse train approximation for ISI requires only one previous pulse because of the rapid fall off in the exponential tails. The difference between the treatment of terms for SS and, say, an optically preamplified system is that all terms are stochastic in SS. This results in a crossproduct term that is the product of two Gaussian distributions, in contrast to a system having a deterministic signal where the relevant term remains Gaussian. Here again the use of the MGF means that this term may be incorporated in the analysis framework without generating a huge computational burden.

The comparison made with recent experimental results in Section V-B shows good agreement and enables predictions of the likely results with integrate and dump filters to be made. The error floor for a single channel system may be reduced by up to two orders of magnitude using integrate and dump filtering. A WDM SS system offers a BER of less than 10^{-8} for 2.5 Gb/s channels. Moreover, these figures are for inexpensive SS systems based only on broad-band sources and FP filters.

The use of a reduced integration time offers a simple technique to reduce the impact of ISI. The relatively slowly rising pulses enable the integration time to be started from as late as 10% of the bit time before the photocurrent is reduced sufficiently to offset the benefits of the ISI reduction. Indeed if the intention was to operate at low m values one could start the integration at 20%–25% of the bit time, since the penalty incurred arises for high m values. The presence of broad minima (Fig. 8) for BER as a function of integration time means that benefits from reduced integration time will accrue even with imprecise control of the starting point.

The results of Figs. 10 and 11 show that it is important that a minimum level of extinction is possible from modulators used in SS systems. However, 20 dB will be sufficient to achieve 10^{-9} BER in most cases and 30 dB offers performance only marginally different from an ideal modulator.

The representative system power budget results in Section VIII demonstrate the effect of using a reduced integration time. A power budget of in excess of 20 dB is available using channels having optical bandwidths of 0.1 nm. Clearly the total transmission capacity available for an SS system depends on acceptable the power budget and BER but seems to be at least tens of gigabits per second.

X. Conclusion

The SPA has been applied to direct detection SS systems for the first time and has provided a tractable approach to BER calculations irrespective of m. Previous analyzes have been extended by the inclusion of pulse distortion by the receiver filter an ISI term and a signal ISI crossproduct term. The limiting factor in SS at low m values has been shown to be these latter terms arising from the exponential tails produced by the receiver FP filter. Severe error floors have been demonstrated that outweigh the eventual power penalty from the noise like nature of the broad-band source. Output from the model has been compared with experimental results giving good agreement and using the 2 FP arrangement for a WDM system suggests BER's

of less than 10^{-8} for 2.5-Gb/s channels. The use of a reduced integration time has been seen to be an extremely powerful, yet simple, technique to reduce the impact of ISI. Control of the starting point for integration need not be overly precise because broad minima are present in the BER versus integration time characteristics. Furthermore, it has been shown that an extinction ratio of 20 dB will suffice for 10^{-9} BER in most cases, with 30 dB offering a performance close to that possible with an ideal modulator. The system power budget may be extended by using reduced integration times and offers the potential for high, low cost system transmission capacity. The SPA may also be used to consider the performance of noise reduction methods and optical preamplification, and this forms the basis of further work by the author.

APPENDIX

The integrated photodiode output may be written as

$$\begin{aligned} I &= \frac{1}{2T}\int_0^T \left[s(t)n(t) + \mathrm{ISI}(t)\right]^2 dt \\ &= \frac{1}{2T}\int_0^T \left[s^2(t)n^2(t) + 2s(t)n(t)\mathrm{ISI}(t) + \mathrm{ISI}^2(t)\right] dt. \end{aligned} \tag{A.1}$$

This produces three terms.

A. Square of the Signal

$$I_1 = \frac{1}{2T}\int_0^T \left(1 - e^{-t/T_c}\right)^2 n^2(t)\, dt. \tag{A.2}$$

Now $n(t)$ is a zero-mean Gaussian random variable, with pdf $f_N(n)$ and spectral density $S_N(f)$ resulting from the filtering of the white spectrum from the noise like (LED) source by two FP filters. However, $s(t)N \equiv N_1$ is not stationary so the standard form of the Wiener–Khintchine Theorem cannot be used. A modification has, however, been derived by Tsao [22] for nonstationary signals. This allows the autocorrelation function to be written, for real $s(t)$, as

$$R_{n_1' t}(\tau) = \int_{-\infty}^{\infty} s(t)s(t-\tau)S_n(f)e^{j2\pi f\tau}\, df. \tag{A.3}$$

Since the PSD is known to be

$$S_n(f) = |H(f)|^4 N_0 \tag{A.4}$$

it follows immediately that

$$\begin{aligned} R_{n_1, t}(\tau) = \frac{\pi N_0 B_{\mathrm{FP}}}{4} &\left(1 - e^{-\pi B_{\mathrm{FP}} t}\right)\left(1 - e^{-\pi B_{\mathrm{FP}}(t-\tau)}\right) \\ &\times \left[1 + \pi|\tau|B_{\mathrm{FP}}\right] e^{-\pi|\tau|B_{\mathrm{FP}}}. \end{aligned} \tag{A.5}$$

The power transmitted may be obtained by considering the autocorrelation function at $\tau = 0$ as $t \to \infty$, i.e., by saying the receiver may collect photons for an infinite time, to give $R_{n_1,\infty}(0) = (\pi N_0 B_{\mathrm{FP}})/4$. Using (16) for the equivalent bandwidth yields the required relationship between the rectangular filter and the FP for meaningful comparison,

$$B_{\mathrm{FP}} = \frac{2.5}{\pi} B_0. \tag{A.6}$$

The eigenvalues used for the KL expansion have a sum equal to $R_{n_1,\infty}(0)$ since the decomposition of the signal is into a sum of zero mean Gaussian random variables with pdf's

$$f_{N_i'}(n_{1i}) = \frac{1}{\sqrt{\pi\gamma_i}} \exp\left(\frac{-n_{1i}^2}{\gamma_i}\right). \tag{A.7}$$

Hence, the eigenvalue equation is

$$\gamma\phi(t) = \int_0^T K_{n_1}(t, u)\phi(u)\, du \tag{A.8}$$

where

$$\begin{aligned} K_{n_1}(t, u) = \sigma^2 &\left(1 - e^{-\pi B_{\mathrm{FP}} t}\right)\left(1 - e^{-\pi B_{\mathrm{FP}} u}\right) \\ &\times \left[1 + \pi|t-u|B_{\mathrm{FP}}\right] e^{-\pi|t-u|B_{\mathrm{FP}}}. \end{aligned}$$

The KL expansion is *not* restricted to stationary signals and so the solution of the nonstationary system may be used to express I_1 thus

$$I_1 \approx \sum_{i=1}^{N_i} n_i^2 \tag{A.9}$$

with N_i large enough to give the required numerical accuracy. The evaluation of $E[\exp(sI_1)]$ provides the required MGF

$$F_{N'}(s) = \prod_{i=1}^{N_i} \frac{1}{\sqrt{1 - s\gamma_i}} \tag{A.10}$$

for each polarization and quadrature component.

B. ISI

The ISI results from the sum of the tails of preceding pulses and thus has the form

$$\begin{aligned} &\left(1 - e^{-T/T_c}\right) e^{-t/T_c} \sum_{k=0}^{\infty} a_{-(k+1)}\, e^{-kT/T_c}\, n(kT) \\ &\quad = \left(1 - e^{-2.5m}\right) e^{-2.5mt/T} \sum_{k=0}^{\infty} a_{-(k+1)}\, e^{-2.5km}\, n(kT) \end{aligned} \tag{A.11}$$

where

- a_i random variable with a 50% probability of being "1" or "0";
- $n(kT)$ samples of the zero-mean Gaussian random variable $n(t)$, with variance $\sigma^2/2$ to account for the premultiplication of (A.1) by $1/2T$.

This series may be dealt with by truncation considering all the possible bit combinations for the number of previous bits retained. Since the sum of two Gaussian random variables is also

Gaussian it is possible to deduce that when all the previous bits are "1" the maximum ISI will be Gaussian with variance

$$\left(1-e^{-2.5m}\right)^2 e^{-5mt/T}\frac{\sigma^2}{2}\sum_{k=0}^{\infty}e^{-5km}. \tag{A.12}$$

Even with the lowest B_0T value considered $(m=1)$ the second and subsequent terms in the series will be of magnitude less than $\exp(-5)=6.7\times10^{-3}$. Hence it is only necessary to consider one previous bit because the accuracy obtained, for considerable extra calculation, will be small if more are retained.

The value of the integral of the ISI is thus

$$\begin{aligned} I_2 &= \frac{1}{2T}\int_0^T \mathrm{ISI}^2(t)\,dt \\ &= \frac{1}{10m}\left(1-e^{-2.5m}\right)^2\left(1-e^{-5m}\right)\chi^2(0) \end{aligned} \tag{A.13}$$

where $\chi^2(0)$ is a chi-squared variable resulting from the squaring of $n(t)$. Note that the $n(kT)$ do not vary with time when the subsequent bit is considered, since they are samples, and thus the integration with respect to t may be performed. The MGF for $\chi^2(0)$ is given by

$$F_{\mathrm{ISI}}(s)=\frac{1}{\sqrt{(1-2k_{\mathrm{ISI}}\sigma^2 s)}} \tag{A.14}$$

for each polarization and quadrature component, where

$$k_{\mathrm{ISI}}=\frac{1}{10m}\left(1-e^{-2.5m}\right)^2\left(1-e^{-5m}\right).$$

C. Cross Product

The cross product

$$I_3=\frac{1}{T}\int_0^T s(t)n(t)\mathrm{ISI}(t)\,dt \tag{A.15}$$

only occurs when both the signal and the ISI are nonzero. Given the approximation made in Section B of the Appendix above the integral may be rewritten as

$$\begin{aligned} I_3 &= \frac{1}{T}\int_0^T\left(1-e^{-2.5mt/T}\right)e^{-0.52mt/T}n(t)\,dt \\ &\quad\times n(0)\left(1-e^{-2.5m}\right) \\ &= X_1X_2 \\ &\equiv X. \end{aligned} \tag{A.16}$$

The random variable X_1 is nonstationary but is Gaussian, since only linear operations are performed on $n(t)$ to obtain it; X_2 is clearly also Gaussian. The product of two Gaussian random variables is known to have zero mean and a pdf [23]

$$f_X(x)=\frac{1}{\pi\sigma_1\sigma_2}K_0\left(\frac{|x|}{\sigma_1\sigma_2}\right) \tag{A.17}$$

where $K_0(\cdot)$ is an order zero modified Bessel function of the second kind. Such an expression may be dealt with using the Mellin transform [24] enabling its variance to be obtained as $(\sigma_1\sigma_2)^2$ and an approximate MGF to order s^2 to be written, for each polarization and quadrature component, as

$$F_X(s)\approx 1+(\sigma_1\sigma_2)^2\frac{s^2}{2}. \tag{A.18}$$

The variance of X_2 may easily be found as $\sigma_2^2=\sigma^2(1-e^{-2.5m})^2$ and X_1 may be approached using the method for nonstationary signals in Section A of the Appendix above to give a variance, after considerable manipulation, of

$$\sigma_1^2\approx\frac{0.028}{m^2}\sigma^2. \tag{A.19}$$

The contribution to the number of photons required to achieve a given BER is generally small, a few percent at most, and becomes negligible as m increases because X remains zero mean and typically $\sigma_1^2,\ \sigma_2^2\ll\sigma^2$.

REFERENCES

[1] J. M. Senior, M. R. Handley, and M. S. Leeson, "Developments in wavelength division multiple access networking," *IEEE Commun. Mag.*, vol. 36, pp. 28–36, Dec. 1998.

[2] J. S. Lee, Y. C. Chung, and D. J. DiGiovanni, "Spectrum-sliced fiber amplifier light source for multichannel WDM applications," *IEEE Photon. Technol. Lett.*, vol. 5, pp. 1458–1461, Dec. 1993.

[3] D. D. Sampson and W. T. Holloway, "100 mW spectrally-uniform broadband ASE source for spectrum-sliced WDM systems," *Electron. Lett.*, vol. 30, no. 19, pp. 1611–1612, 1994.

[4] A. J. Keating and D. D. Sampson, "Reduction of excess intensity noise in spectrum-sliced incoherent light for WDM applications," *J. Lightwave Technol.*, vol. 15, pp. 53–61, Jan. 1997.

[5] D. K. Jung, S. K. Shin, C.-H. Lee, and Y. C. Chung, "Wavelength-division multiplexed passive optical network based on spectrum-slicing techniques," *IEEE Photon. Technol. Lett.*, vol. 10, pp. 1334–1336, Sept. 1998.

[6] V. Arya and I. Jacobs, "Optical preamplifier receiver for spectrum-sliced WDM," *J. Lightwave Technol.*, vol. 15, pp. 576–583, Apr. 1997.

[7] G. Einarsson, *Principles of Lightwave Communications*. New York: Wiley, 1996.

[8] J. G. Proakis, *Digital Communications*. New York: McGraw-Hill, 1995.

[9] H. L. Van Trees, *Detection Estimation and Modulation Theory—Part I.* New York: Wiley, 1968.

[10] P. A. Humblet and M. Azizoglu, "On the bit error rate of lightwave systems with optical amplifiers," *J. Lightwave Technol.*, vol. 9, pp. 1576–1582, Nov. 1991.

[11] I. T. Monroy and G. Einarsson, "Bit error evaluation of optically preamplified direct detection receivers with Fabry–Perot optical filters," *J. Lightwave Technol.*, vol. 15, pp. 1546–1553, Aug. 1997.

[12] S. Herbst, P. Meissner, M. Baussman, and M. Erbasch, "Sensitivity of a direct WDM-system with a frequency selective optical receiver and optical preamplifier," *J. Lightwave Technol.*, vol. 16, pp. 32–36, Jan. 1998.

[13] C. Lawetz and J. C. Cartledge, "Performance of optically preamplified receivers with Fabry–Perot filters," *J. Lightwave Technol.*, vol. 14, no. 11, pp. 2467–2474, 1996.

[14] J.-S. Lee, "Signal-to-noise ratio of spectrum-slice incoherent light sources including optical modulation effects," *J. Lightwave Technol.*, vol. 14, pp. 2197–2201, Oct. 1996.

[15] M. S. Leeson, "A fast approximation for bit error rate calculations in optically preamplified receivers," *Electron. Lett.*, vol. 33, no. 15, pp. 1329–1330, 1997.

[16] S. R. Chinn, "Error-rate performance of optical amplifiers with Fabry–Perot filters," *Electron. Lett.*, vol. 31, no. 9, pp. 756–757, 1995.

[17] D. Ben-Eli, E. D. Yeheskel, and S. Shamai (Shitz), "Performance bounds and cutoff rates of quantum limited OOK with optical amplification," *IEEE J. Select. Areas Commun.*, vol. 13, pp. 510–530, Apr. 1995.
[18] L. F. B. Ribiero, J. R. F Da Rocha, and J. L. Pinto, "Performance evaluation of EDFA preamplified receivers taking into account intersymbol interference," *J. Lightwave Technol.*, vol. 13, pp. 225–232, Feb. 1995.
[19] V. Arya, "Analysis design and performance evaluation of optical fiber spectrum-sliced WDM systems," Ph.D. dissertation, Virginia Polytech. Inst. State Univ., Blacksburg, VA, 1997.
[20] S. D. Personick, "Statistics of a general class of avalanche detectors with applications to optical communication," *Bell Syst. Tech. J.*, vol. 50, pp. 3075–3095.
[21] G. P. Agrawal, *Fiber-Optic Communication Systems*. New York: Wiley, 1997.
[22] Y. H. Tsao, "Spectral model and time-varying covariance functions for the nonstationary processes," *J. Acoust. Soc. Amer.*, vol. 76, no. 5, pp. 1422–1426, 1984.
[23] M. D. Springer, *The Algebra of Random Variables*. New York: Wiley, 1979.
[24] B. Epstein, "Some applications of the Mellin transform in statistics," *Ann. Math. Stat.*, vol. 19, pp. 370–379, 1948.

Mark S. Leeson received the degree (with First Class Honors) in electrical and electronic engineering from the University of Nottingham,U.K., in 1986 and the Ph.D. degree in novel optical modulators in the Engineering Department from the University of Cambridge, U.K., in 1990.

From 1990 to 1992, he worked in the IT Division of a large United Kingdom bank carrying out communication network simulations. He then held lecturing appointments in London, U.K., and Manchester, U.K., prior to joining the Department of Electronic and Computer Engineering, Brunel University, Uxbridge, Middlesex, U.K., in September 1998. His research interests cover optical receivers, optical devices, communication protocols, optical wavelength conversion, and error correcting codes. He has published 35 journal and conference papers and is a Chartered Engineer.

Dr. Leeson is a member of the Institution of Electrical Engineers (IEE) in the United Kingdom. He has acted as a referee and reviewer for several journals, including the *IEE Proceedings* and *Electronics Letters*, and been a member of both SPIE and IEEE conference program committees.